AD 274 498

ARL 131

274 498

ELECTRONIC PROPERTIES OF SOME INTERMETALLIC COMPOUNDS

E. MILLER
B. SEIDMAN
O. KOMAREK
I. CADOFF

NEW YORK UNIVERSITY
NEW YORK, NEW YORK

DECEMBER 1961

AERONAUTICAL RESEARCH LABORATORY
OFFICE OF AEROSPACE RESEARCH
UNITED STATES AIR FORCE

NOTICES

When Government drawings, specifications, or other data are used for any purpose other than in connection with a definitely related Government procurement operation, the United States Government thereby incurs no responsibility nor any obligation whatsoever; and the fact that the Government may have formulated, furnished, or in any way supplied the said drawings, specifications, or other data, is not to be regarded by implication or otherwise as in any manner licensing the holder or any other person or corporation, or conveying any rights or permission to manufacture, use, or sell any patented invention that may in any way be related thereto.

Qualified requesters may obtain copies of this report from the Armed Services Technical Information Agency, (ASTIA), Arlington Hall Station, Arlington 12, Virginia.

This report has been released to the Office of Technical Services, U. S. Department of Commerce, Washington 25, D. C. for sale to the general public.

Copies of ARL Technical Reports and Technical Notes should not be returned to Aeronautical Research Laboratory unless return is required by security considerations, contractual obligations, or notices on a specific document.

ARL 131

ELECTRONIC PROPERTIES OF SOME INTERMETALLIC COMPOUNDS

E MILLER
D SEIDMAN
K KOMAREK
I CADOFF

NEW YORK UNIVERSITY
NEW YORK, NEW YORK

DECEMBER 1961

CONTRACT AF 33(616)-8363
PROJECT 7021
TASK 70661

AERONAUTICAL RESEARCH LABORATORY
OFFICE OF AEROSPACE RESEARCH
UNITED STATES AIR FORCE
WRIGHT-PATTERSON AIR FORCE BASE, OHIO

300 - April 1962 - 27-1129 & 1130

FOREWORD

This final report was prepared by New York University under USAF Contract AF 33(616)-3883. This contract was initiated under Project 7021 "Solid State Research and Properties of Matter", Task 70661 "Effects of Internal Structure and Impurities on the Conductivity and Allied Phenomena in Solids". The work was administered under the direction of the Aeronautical Research Laboratory, Office of Aerospace Research, Wright-Patterson Air Force Base, Ohio. Mr. J. W. Poynter was the project engineer.

A major portion of the work carried out under this contract has been described in ARL Technical Report 59-570, dated October 1960, and in three publications which have appeared in the Transactions of the AIME. Reference to these publications is cited in the body of the report. This final report summarizes the additional work carried out in the period January 1960 through May 1961 which has not as yet been published.

ABSTRACT

An investigation of the physical and electronic properties of PbTe, PbSe, BaTe, BaSe, and alloys of the system $Pb_xSn_{(1-x)}Te$ was carried out. A major portion of the work on PbTe appeared previously in ARL Technical Report 59-570.

Additional analysis of the data for the PbTe system shows that the disparity in energy gap values for PbTe as determined from optical and thermal measurements may be explained by generation of excess carriers due to defect generation at elevated temperatures. An analysis of activation processes involved points to Pb interstitials as the most likely defect present.

BaSe and BaTe can be prepared by direct reaction of Ba with Se and Te. The binding energies of these compounds is high as evidenced by their high melting points, and high resistivity at room temperatures, indicating that both would have rather high energy gaps. On examination of the PbSe phase diagram by thermal analysis and metallographic techniques it was determined that:

1) the melting point of PbSe is 678.3°C,

2) a monotectic reaction occurs on the selenium rich side of PbSe, but

does not occur on the lead rich side of PbSe.

Measurements of electronic properties of PbSe indicated that,

1) stoichiometric PbSe does not melt at the maximum melting point but the maximum melting point occurs at a composition containing 0.009 atomic percent selenium.

2) the energy gap as determined from resistivity and Hall effect as a function of temperature greater than that reported from optical measurements.

3) on the basis of exploratory quenching experiments, it appears that the above discrepancy results from defect generation, as in the case of PbTe.

PbTe and SnTe are completely miscible in the system $Pb_xSn_{(1-x)}Te$. Preliminary experiments indicated that the electronic parameters vary continuously as Sn is substituted for Pb.

TABLE OF CONTENTS

LIST OF ILLUSTRATIONS

LIST OF TABLES

I. INTRODUCTION

The electronic properties of lead telluride and several related compounds; lead selenide, barium telluride, barium selenide, and tin telluride have been investigated for application in thermoelectric circuits.

The early work on lead telluride was reported in ARL Technical Report 59-570. At that time it was observed that a significant discrepancy existed between the energy gap values for PbTe determined from optical measurements as compared with that determined from temperature excitation of electron hole pairs. As described in a later section, the optical value is the proper one to use, the thermal value being affected by the generation of lattice defects.

Work on BaSe and BaTe was published in the Transactions of AIME (1). The major conclusions are summarized in a later section.

Investigation of PbSe lead to observations similar to those found in the PbTe system:

a) the maximum melting point of PbSe does not coincide with the stoichiometric point

b) generation of defects results in a discrepancy between optical and thermal energy gap values

In addition, the lead rich portion of the Pb-Se phase diagram was reinvestigated.

The study of SnTe and PbTe-SnTe alloys did not reach the point where significant results can be reported. However, the preliminary observations are summarized in the body of the report.

II. INTERRELATION OF ELECTRONIC PROPERTIES AND DEFECT EQUILIBRIA IN PbTe

The resistivity, Hall coefficient a[illegible]ebeck coefficient of single crystals of PbTe were investigated in the range from 77°K to 900°K using a capsuling arrangement which prevented tellurium loss from the specimens at elevated temperatures. The low temperature properties obtained agree with the data reported in the literature. The thermal energy gap obtained from the high temperature measurements could not however be brought into agreement with the energy gap determined from room temperature absorption measurements by considering solely the excitation

---

Manuscript released by authors 1 June 1961 for publication as a WADD Technical Report

of electron-hole pairs across the energy gap at elevated temperatures. Rather, it is necessary to include the carriers generated by defect formation at elevated temperatures. Both Schottky-Wagner and Frenkel defects are present, the activation energies for formation of the two types of defects being related by the equation:

(1) $$E_F = 1/2\ E_S + 0.55eV \cong 0.7eV$$

The possible occurrence of such discrepancies has been discussed by Smith (2), who concluded that they can be attributed either to unusual changes in the band structure of the compound with temperature, to vaporization of tellurium and/or to the formation of defects at elevated temperatures.

Since the discrepancy between optical and thermal energy gap values has not yet been completely resolved, the purpose of the present investigation was to redetermine the electronic properties of the compound using a capsulating technique which would completely eliminate tellurium losses at elevated temperatures during measurements, and to compare these data with room temperature optical data.

The results reported in TR59-570 show that the energy gap calculated from measurements of resistivity as a function of temperature is indeed considerably greater than that obtained from optical absorption experiments, even when tellurium vaporization is completely suppressed. The experimental results show that marked variation of the basic electronic parameters with temperature unlikely, and that this mechanism cannot be used to explain the discrepancy. However, quenching experiments indicate that defects present at elevated temperatures create additional carriers in PbTe, and that such carrier generation can satisfactorily explain the disparity between the optical and thermal energy gaps. While Smith considered that defects were produced at elevated temperatures primarily as a result of vaporization of tellurium from the specimens, our data indicate that the lattice defects that predominantly affect the electronic properties are lead interstitial ions. The energy of formation of the interstitials can be calculated from the electronic data, and the analysis is presented in the following discussion.

The energy gap of a semiconductor is generally obtained by one of the following three methods:

1. Determination of the absorption edge; that is, the minimum value of photon energy which is absorbed after correction for free carrier absorption.

2. From conductivity vs temperature measurements. If the specimens can be assumed to be intrinsic, then:

(2) $$\sigma = 2(2\pi kT)^{3/2} (m_e m_h)^{3/4} (\mu_n + \mu_p) \exp - (E/2kT)$$

or

$$(3) \quad \sigma = AT^{3/2} (\mu_n + \mu_p) \exp - (E_o/2kT)$$

where A is a constant depending on the shape of the energy contours, effective masses and temperature variation of the energy gap. If

$$(4) \quad \mu = cT^{-3/2} ,$$

then the slope of a ln σ vs I/T plot should yield the energy gap at 0°K.

3. From Hall coefficient vs temperature measurements: If the specimen is either in the transition or intrinsic region the Hall coefficient can be given by:

$$(5) \qquad R = r(nb^2 - p)/(nb + p)^2 e$$

Where r depends on the shape of the energy contours and the statistics obeyed by the charge carriers, and b is the mobility ratio.

The usual analysis is to set: $n - p = N_D$ in the transition region and $n = p$ in the intrinsic region, where N_D is the impurity concentration. Then since:

$$(6) \qquad npT^{-3} = B \exp -(E_o/kT)$$

the slope of a ln npT^{-3} vs I/T plot should give the energy gap at 0°K.

However, direct application of these standard equations to the data has resulted in definite discrepancies. The optical value of the energy gap extrapolated to 0°K is 0.17 eV, while the best slope of the ln σ vs I/T curve is 0.35 eV. Similar discrepancies have been observed in the homologous compounds PbS and PbSe. The optical and thermal energy gaps for PbS are 0.22 (3) and 0.32 eV (4), and for PbSe 0.15 (3) and 0.48 eV (5). In addition, it is quite surprising that a straight line can be drawn through the elevated temperature conductivity data since it is seen that above 300°K, the mobility dependence on temperature is $T^{-5/2}$. If this region is the true intrinsic region, the conductivity line should definitely curve concave upward. It is shown later that the conductivity in this region is controlled by defects.

While such differences have been mainly discounted in previous work as the result of composition change at elevated temperatures (4), the observed reproducibility of the data after extended heating times indicates that no significant composition change occurred, and therefore the discrepancies observed are real effects.

As has been stated by Smith (2), the thermally determined value of the energy gap will yield the true energy gap at 0°K only if

the energy gap varies linearly with temperature, and the factors A in equation 3 and B in equation 6 are constant (implying m* and b are independent of temperature).

If the bandgap is quadratically dependent on T, then the energy gap can be written as:

$$E = E_o + \beta T - \gamma T^2 \tag{7}$$

and the energy gap calculated from the slope of the ln σ vs I/T curve will actually be (2):

$$E = E_o + \gamma T^2. \tag{8}$$

The energy gap of PbTe as a function of temperature has been plotted by Smith (2) from the infrared absorption data of Gibson (6) Although there is some curvature to the graph, the effect on the measured bandgap due to the curvature as calculated by equation 8 is only about 0.07 eV.

With regard to the possible variation of the factor A in equation 3, the Seebeck coefficient data obtained gives a constant effective mass from 77°K to 300°K. Even more conclusive proof of the constancy of the effective mass is the thermoelectric data of Kolomoets et al (7), who observed no change in the effective mass over the wide temperature range from 0° to 450°C. This temperature interval includes most of the region over which the intrinsic resistivity data for our study was taken, and variation of the pre-exponential factor can therefore be considered negligible. Therefore, the other possibility suggested by Smith must be considered, that is, the generation of defects at elevated temperatures.

Measurements taken as a function of temperature will in this case detect carriers generated by two distinct mechanisms: 1) the excitation of electron-hole pairs and 2) the formation of structural defects at elevated temperatures and the ionization of their isolated energy levels. Optical measurements at room temperature, on the other hand, will only generate carriers by mechanism 1.

The data obtained from quenching experiments indicate that carriers are generated due to defect formation at elevated temperatures. Two temperature ranges can be observed. In the temperature interval from 500 - 800°K, the carrier concentration of both the n and p types samples increases while above the upper temperature the carrier concentration of the n-type sample continues to rise, while that of the p-type sample begins to fall.

The lower temperature range has been studied previously. Koval'chick and Maslakovets (8) obtained an activation energy for the production of carriers of 0.62 eV in p-type material assuming a bimolecular

reaction (0.31 eV slope). They stated that the production of carriers during annealing is caused by the solution of excess quiescent impurity atoms. Fritts (9) obtained a slope of 0.55 eV in both n- and p- type material. He concluded that both lead and tellurium show retrograde solubility in PbTe. Such retrograde solubility has been reported for PbTe (10).

However, in the temperature range above 800°K, the concentration of electrons in both n and p-type samples after quenching begins to increase. The carriers therefore apparently come from the generation of structural defects, which is independent of the small composition difference of the two samples.

If, as will be proposed later, the structural defects produced at elevated temperatures which cause significant changes in the electronic properties are lead interstitial atoms, then migration and recombination of the interstitials with lead vacancies would be expected to be fairly rapid, even at relatively low temperatures (11). Only on quenching from elevated temperatures, where their concentrations are relatively high would a measurable concentration of interstitials be expected to be trapped. In the lower temperature range the excess lead or tellurium atoms dissolved in the lattice due to retrograde solubility which are substitutional and which therefore cannot migrate as rapidly as the interstitials would be quenched in and would control the room temperature electronic properties.

If the increase in carrier concentration due to retrograde solubility were the only source of additional carriers, then in p-type material the conductivity would be given at elevated temperatures by:

$$\sigma = (n + p_{re})\, e\mu_p + ne\mu_n = (n[b + 1] + p_{re})e\mu_p$$

where p_{re} = no. of carriers /cm^3 due to increasing solubility with increasing temperature and n = no. of electrons excited across the energy gap.

At any temperature:

$$(n = p_{re})\, n = n_i^2$$

If we take the mobility as being given by:

$$\mu_p = dT^{-5/2} \quad \text{and} \quad b = \mu_n/\mu_p = 2.1$$

then solving for the number of excess carriers gives:

$$\sigma = \left[-0.55\, p_{re} + 1.55\, (p_{re}^2 + 4n_i^2)^{1/2}\right] ecT^{-5/2}$$

or:

$$p_{re} = \frac{0.71\,\sigma cT^{5/2} + (4\sigma^2 T^5 c^2 - 14 n_i^2)^{1/2}}{1.75} \qquad (9)$$

where $c = 0.645/ed$. While the value of n_i^2 is unknown, its temperature dependence must be $CT^3 \exp(-0.17/kT)$ (using the energy gap obtained from the infrared absorption measurements). Substituting the experimental values for c and σ, then regardless of what reasonable value of c is chosen (to make $n_i = 10^{15}$ to 10^{18} at room temperature) solution of eq. 9 shows that the concentration of additional carriers at 600°K and above must be significantly greater than that generated by intrinsic electron-hole pair excitation, and the latter may be neglected with little error.

Considering retrograde solubility only, since the concentration of additional carriers is greater than that from electron-hole excitation, the Seebeck coefficient of p-type material should remain positive in sign for all temperatures. Since the Seebeck coefficient is negative above 500°K for all samples, the number of carriers introduced by retrograde solubility must be fairly small compared to that produced by lattice defects and need not be considered at elevated temperatures, contradicting the suggestion by Fritts and Karrer (12).

DEFECT FORMATION ENERGY

The calculation based on equation 9, and the fact that the Seebeck coefficient is n-type for all samples at elevated temperatures, indicate that above 600°K thermally generated n type defect centers become controlling. The conductivity-temperature curves at these temperatures can be used to determine the activation energy for defect formation. For n-type carriers predominating, we have:

$$\sigma = n' e \mu_n$$

where n' is the number of carriers due to defect formation. Since above room temperature the mobility can be written as:

$$\mu_n = c' T^{5/2}$$

then σ can be written as:

$$\sigma = D \exp -(E_n/kT)\, T^{-5/2}$$

This equation can be fitted to the conductivity data for $E_n = 0.31$ eV over the entire intrinsic temperature range studied. Therefore

$$n' = F \exp -(0.31/kT) \qquad (10)$$

There is relatively little data on the types of defects present in PbTe and their energies of formation. The activation energy for diffusion of Pb and Te in PbTe was obtained by Boltaks and Makhov (13) as 0.6 and 0.75 eV respectively. The low value of the activation energy suggests an interstitial diffusion mechanism, but since the activation energy for diffusion of both Pb and Te are close, and the radius of the $Te^{=}$ ion is too large to permit interstitial migration, they concluded that the mechanism must be one of vacancy migration.

Defects that will result in energy levels in the forbidden band can either be Frenkel defects, Schottky-Wagner defects or anti-structure disorder (14). While anti-structure disorder is possible, such defects are extremely unlikely to occur in polar compounds and this type of defect can be ignored. If both Schottky-Wagner and Frenkel defects exist in PbTe, then Te vacancies, Pb vacancies and Pb interstitials will be present. Due to the large ionic radius of the Te ion, the concentration of Te interstitials will be very small and can be neglected. The Hall effect data indicate that the ionization energy of the defects is quite small, and we can conclude that the first ionizations of the defects occur with an extremely low activation energy, while second ionizations do not occur.

The interactions involving the various defects consist of the formation of the lead vacancies and interstitials, the tellurium vacancies, the ionization of these defects and the generation of electrons and holes by excitation across the forbidden band. The charge on the various components is written below with respect to the lattice, so that the ordered lattice is designated by the neutral symbol PbTe. The charge of the vacancies is therefore opposite that of the lattice site occupied by its normal ion. In this convention a lead ion sitting on a lead site is uncharged with respect to the lattice, while a lead interstitial will be doubly positively charged and a lead vacancy doubly negatively charged. The equations denoting the first ionizations of the various defects follow directly from the apparent charges on the defects. In setting up these equations it is important to note that as a result of the encapsulation the composition of the crystal is constant, and does not vary as a function of temperature. This requirement is specified in equations 17 and 18.

The various equilibria involving the different defects and the charge carriers can therefore be written as:

(11) ground state $= n^{-} + p^{+}$ $\qquad K_1 = [n^{-}][p^{+}] = n_i^2$

(12) $PbTe = V_P^{=} + V_T^{++}$ $\qquad K_2 = [V_P^{=}][V_T^{++}]$

(13) $Pb = I_P^{++} + V_P^{=}$ $\qquad K_3 = [I_P^{++}][V_P^{=}]$

(14) $I_P^{++} = I_P^{+} + p^{+}$ $\qquad K_4 = \dfrac{[p^+]\,[I_P^+]}{[I_P^{++}]}$

(15) $V_P^{=} = V_P^{-} + n^{-}$ $\qquad K_5 = \dfrac{[V_P^-]\,[n^-]}{[V_P^=]}$

(16) $V_T^{++} = V_T^{+} + p^{+}$ $\qquad K_6 = \dfrac{[V_T^+]\,[p^+]}{[V_T^{++}]}$

The electroneutrality condition is:

(17) $[n^-] - [p^+] + [V_P^-] - [V_T^+] - [I_P^+] - 2[I_P^{++}] - 2[V_T^{++}] + 2[V_P^=] = 0$

and the requirement that the composition remains unchanged by defect formation is:

(18) $[I_P^{++}] + [I_P^+] = [V_P^-] + [V_P^=] - [V_T^{++}] - [V_T^+]$

These equations can be solved using the approach suggested by Brouwer (15), by obtaining simplified electroneutrality and composition equations.

It was shown from Equation 9 that $n \gg p$, and therefore the hole concentration can be neglected in Equation 17, as can the concentration of doubly charged vacancies in eq. 18 as well as eq. 17. Then:

(17B) $[n^-] = 2[I_P^{++}] + [I_P^+] - [V_P^-] + [V_T^+]$

If $[I_P^{++}] = 0$, complete compensation of the various defects occurs, and $[n^-] = 0$. This limiting case is therefore impossible. The other limit is to let $[I_P^+] = 0$, that is, to consider the case where the interstitial lead atoms have a large ionization energy.

If $[I_P^+] = 0$, then from Equation 18

$$[I_P^{++}] = [V_P^-] - [V_T^+]$$

The simplified electroneutrality condition is:

(17C) $[n^-] = [I_P^{++}]$

Equation 18 can also be simplified. From the diffusion experiments of Boltaks and Makhov we can conclude that $[I_P^{++}] + [I_P^{+}] \ll [V_P^{+}]$ and can be neglected.

Equation 18 simplifies to:

$$[V_P^{-}] - [V_T^{+}] = 0 \qquad (18B)$$

The equations governing the equilibria are therefore Equations 11 - 16 and Equations 17C and 18B. Solving these eight simultaneous equations for the concentration of electrons yields:

$$[n^{-}] = F \exp(-E_O + E_S + E_{IT} - 2E_F - E_{IP})/4kT \qquad (19)$$

E_{IT} and E_{IP} are very small, $E_S = 0.17$ eV and from eq. 10 $[n^{-}]$ varies experimentally as exp $-(0.31/kT)$. Substituting these quantities into eq. 19 yields:

$$E_F = 0.55 + 1/2\, E_S \qquad (20)$$

The energies of formation of Frenkel and Schottky defects are therefore related. The small energy of formation of both these defects is probably due to the unusually high polarizability of the Pb^{++} and $Te^{=}$ ions, which permits coulombic relaxation to reduce the energy of the defects once formed.

E_S can be estimated to be approximately one-half the activation energy of diffusion (0.6 eV) so that

$$E_F \approx 0.7 \text{ eV}$$

The activation energy for movement of a Frenkel defect can be taken to be very roughly one-half that of movement of a Schottky defect (14) so that the activation energy for diffusion of a Frenkel defect is:

$$D_F \approx 0.8 - 0.9 \text{ eV}$$

The larger energy of formation of Frenkel defects indicates that the concentration of these defects is significantly less than that of the Schottky defects. This therefore corroborates the assumption of Boltaks and Makhov that diffusion is essentially controlled by a vacancy mechanism.

III. PROPERTIES OF BaTe AND BaSe

The high mean atomic weight and possible high value of energy gap were the attractive features of BaTe and BaSe. However, high purity compounds are difficult to obtain because of the reactivity of barium with the atmosphere and the large heats of formation of the compounds.

A. Preparation of BaTe and BaSe:

The compounds were prepared by direct reaction of the two elements. Purified barium and semiconductor grade tellurium and selenium (99.999+ pct) were used as the starting materials. Since tellurium and selenium react with metals, and barium tends to reduce refractory oxides, high purity reactor grade graphite crucibles were used. The crucibles were outgassed in vacuum at 1000°C for 4 hr prior to use. The crucibles were charged with the reactants and then sealed separately into iron bombs in an argon atmosphere dry box. The bomb was then placed in a furnace and heated in vacuum to the melting point of tellurium or selenium. Rapid reaction occurred upon melting, and the heat of formation raised the temperature above the melting point of the compound. Sound nonporous polycrystalline ingots were obtained.

B. Properties of BaTe and BaSe:

Debye-Scherrer powder diffraction patterns, taken in a 114.6 mm diameter camera using filtered CuKα radiation, confirmed the B1 (NaCl) structure for both compounds. The lattice parameters obtained were $a_o = 7.004 \pm 0.002$Å for BaTe and $a_o = 6.600 \pm 0.002$Å for BaSe. These values can be compared with those reported by Goldschmidt (16): $a_o = 6.99$Å for BaTe and $a_o = 6.58$Å for BaSe. The ionic radii of nitrogen and oxygen are smaller than those of tellurium and selenium, so that solution of these impurities in the compounds would tend to reduce the lattice constant. The higher values obtained in the present investigation can therefore be attributed to higher purity. No extraneous lines were found in the X-ray pattern, indicating that carbon pickup during reaction was insignificant.

The melting points of the compounds were determined by direct visual observation. Specimens weighing about 1 g were placed on a tungsten strip resistance heater in an evacuated chamber (17) and melting was observed through a quartz window. In vacuum, both the BaTe and BaSe specimens evaporated completely in less than 15 sec at 1300°C. Introduction of argon corresponding to 600 mm Hg at temperature retarded vaporization sufficiently to permit observation of the sample for several minutes. In addition to direct sighting through an optical pyrometer the melting point of the sample was determined by comparison with those of elements placed on the heater next to the compound. The melting point of BaTe as measured with the optical pyrometer was 1500° ± 50°C. BaTe remained solid at the melting point of cobalt (1480°C) but was observed to melt

before iron (1535°C). The melting point of BaSe, obtained by means of pyrometer sightings, was 1850° ± 75°C. Comparative observations placed the melting point between that of platinum (1773°C) and zirconium (1857°C); melting of BaSe occurring almost simultaneously with zirconium. On the basis of these observations the respective melting points of BaTe and BaSe were fixed at 1510° ± 30°C and 1830° ± 50°C.

The electrical resistivity for a BaTe and a BaSe specimen was determined as a function of temperature using the two probe method. A Kepco dc constant voltage supply was the power source and the current through the sample was measured with a Millivac micro-microammeter. To eliminate current leakage through the alumina insulation at elevated temperatures, the insulation was preheated at 1000°C for 8 hr. To exclude the possibility of thermionic emission from the sample, the specimen was placed at 90 v positive with respect to ground. The room-temperature resistivity of the samples was highly dependent upon conducting moisture and hydroxide layers on the surface; the samples were therefore heated for four hours at 400°C in vacuum to convert these layers to nonconducting oxides.

The variation of resistivity with temperature in the range from 300° to 830°K is shown in Fig. 1. The room-temperature resistivity of the BaTe specimen was 7×10^7 ohm-cm and that of the BaSe sample was 3×10^{10} ohm-cm.

The graph shows a continuously increasing slope with increasing temperature. According to Pell (18) the carrier mobility of BaO increases from about 3 cm^2/v-sec at low temperatures to about 5 cm^2/v-sec at high temperatures. If we assume that the variation of mobility with temperature for BaSe and BaTe will not be greatly different from that of BaO, we can conclude that the large decrease in resistivity with increase in temperature must be due to an increase in carrier concentration.

The large room temperature resistivities suggest that the bandgaps are large, consistent with the optical absorption and photoemission data of Zollweg (19) which indicate that the bandgaps of BaTe and BaSe are of the order of several electron volts; the conductivity observed must therefore be due to ionized impurities. Because of the curvature of the log resistivity vs 1/T graph, a definite ionization energy could not be calculated, but from the slope of the curve at low temperatures, the impurity ionization is of the order of 0.25 ev.

The high values for resistivity and Eg coupled with purification problems do not make BaTe and BaSe attractive semiconductor materials for low temperature applications but they are potential high temperature materials.

IV. THE Pb-Se SYSTEM

Phase relations in the Pb-Se system and some electronic properties of PbSe were investigated. The experimental techniques used are essentially the same as those reported for the PbTe study in TR 59-570.

A. Liquidus of the Pb-Se Phase Diagram in the Region 30-70 Atomic Percent Selenium:

The liquidus was determined from direct thermal analysis by the study of the freezing curves for sixteen different compositions. In Table I a list of the compositions studied will be found along with the cooling rate employed in each analysis. The EMF observed at the freezing point was converted to degrees centigrade by using the quadratic equation determined in the calibration of the thermocouple. Data showing excessive supercooling were rejected in favor of curves with slight or no supercooling.

One monotectic reaction was found to occur at 76.5 atomic percent selenium. This value is in agreement with the activity measurements of Nozato and Igaki (20). The temperature of this invariant reaction was found to be 678.3°C. See Table II for a summary of the data.

Figure 2 shows the liquidus in the immediate vicinity of the stoichiometric composition, while Figure 3 shows the liquidus and the monotectic reaction in the composition range from 30 to 70 atomic percent selenium. The maximum melting temperature was determined to be 1080.7°C.

B. Observations on the Lead Rich Portion of the Pb-Se Phase Diagram:

In the region between 50 and 100 atomic percent lead, the literature is in disagreement as to whether or not a monotectic reaction occurs. Pelabon (21) reported a two phase region consisting of lead rich liquid and solid PbSe extending from almost pure lead to the compound PbSe, and gave the melting point of PbSe as 1065°C. The data of Friedrich and Leroux (22) agreed with the phase diagram of Pelabon. They determined the melting point of PbSe to be 1083°C. However, Nozato and Igaki (20) by inverse rate thermal analysis observed a monotectic reaction isotherm existing at 860°C with the monotectic point at 20.5 at % Se. The miscibility gap in the liquid state extends from 7.5 to 20.5 atomic percent selenium. Hansen and Anderko (23) accepted Nozato and Igaki's phase diagram in the region of the Pb rich monotectic.

To reinvestigate this portion of the PbSe phase diagram, both thermal analysis and metallographic examination of various compositions were performed. Cooling curves were obtained on the alloys listed in Table III. Data was taken at cooling rates ranging between one-half to two degrees centigrade per minute. The alloys were heated well above the liquidus and shaken vigorously to insure homogeneity.

No evidence of a break indicative of the monotectic reaction was observed, but rather the liquidus points obtained confirm the two phase region found by Pelabon (21) and Friedrich and Leroux (22). The melting point of stoichiometric PbSe was determined for two samples to be 1080.7 ± 0.5°C.

To complement the thermal analysis data an 86 at % Pb sample was examined microscopically. This composition was in the center of the miscibility gap reported by Nozato and Igaki (20). The alloy was heated to 1000°C, held for 1/2 hr, and water quenched. The specimen was polished using standard metallographic techniques for lead. The alloy was etched with an acetic-nitric acid etchant for 10 minutes at 15°C. Microscopic examination did not indicate the existence of two separate layers or solidified droplets imbedded in a matrix, as would be expected if a miscibility gap were present. The microstructure for a similar alloy, air cooled, shown in Fig. 4 consists of uniformly dispersed, dendritic lead selenide in a lead rich matrix.

Both the thermal analysis and the metallographic study therefore indicate that a monotectic reaction isotherm does not exist in the lead rich portion of the lead selenium system.

C. Deviation of Maximum Melting Point from Stoichiometric PbSe:

Three single crystals were prepared of the following compositions:

1. Stoichiometric PbSe
2. 0.02 Atomic percent excess lead
3. 0.03 Atomic percent excess lead

Resistivity scans of each single crystal were made employing the four point probe technique. Three scans of each crystal were made and the resistivities reported in Table IV are average values. Typical scans can be found in Figures 5-8.

The resistivity data is converted to composition in the following manner.

The number of carriers per cubic centimeter on the solidus is given by the expression.

$$p = 1/\mu_p \rho e \qquad (21)$$

The mobility μ_p was determined in this laboratory by the Hall Effect. The specimen was assumed to have a non-degenerate distribution. Thus the equation used was

$$R_H = \frac{3\pi}{8} \frac{1}{pe} \qquad (22)$$

where experimentally

$$R_H = V_H b / \jmath_H \quad (23)$$

The value obtained for the mobility of holer was 550 cm^2/volt sec where RH is 4.92 cm^3/coulomb for p-type material. The number of holes is obtained from (21).

Figure 9 illustrates the method used to calculate the deviation from stoichiometry. The liquidus curve is given by the overall composition while the solidus is given by the composition calculated from the seed end resistivity. It was assumed that in the small composition range investigated the liquidus and solidus curves could be approximated by straight lines. Thus, one obtains the value of the maximum melting point composition at the intersection of the liquidus and the solidus. The value obtained is 0.009 atomic percent excess selenium. The liquid in equilibrium with stoichiometric lead selenide is 0.08 atomic percent excess lead.

The value of 0.009 is slightly higher than the value of 0.005 excess selenium obtained by Goldberg and Mitchell (24).

The method used above permits only the relative positioning of the liquidus and solidus with respect to composition. The melting ranges must be obtained from thermal analysis data.

D. Electronic Properties of PbSe:

Putley (25) measured the electrical conductivity and Hall effect in the PbS, PbSe, and PbTe series and found that the mobilities in these compounds obeyed a power law of the form $\mu = \mu_0 T^{-5/2}$ where μ_0 is a constant over the range 100°K to 700°K. In a later paper Putley (26) reported intrinsic conduction data which provided additional evidence for the $T^{-5/2}$ mobility variation. From Hall effect data he calculated the energy gap of PbSe, and using the $T^{-5/2}$ mobility variation he was also able to calculate an energy gap value from conductivity data. The values were 0.50 eV and 0.45 eV respectively.

Hirahara and Murakami (5) measured the electrical conductivity and Hall constant of P and n-type lead selenide in the range from 500°C to -180°C. They employed polycrystalline samples prepared by sintering powders of selenium and lead under a pressure of 100/Tg/cm. The high temperature measurements were made in an atmosphere of pure nitrogen gas.

Between 334°K and 500°K Hirahara's data was linear. They assumed this to be the intrinsic region and by plotting log σ versus $1/T$ they obtained an energy gap of 0.48 eV. Additional data reported by Hirahara and Murakami include mobility ratio, $b = \frac{\mu_e}{\mu_h} = 1.43$ from which

the effective mass ratio $\frac{m_e}{m_h} = 1.15$ may be calculated.

E. Electronic Data:

The energy gap was measured on two crystals. One was a single crystal of stoichiometric composition, while the second was a tri-crystal containing an excess of 0.08 lead over the stoichiometric composition.

The crystals were sealed into pyrex capsules and tungsten leads were brought into the capsules via glass to metal seals. The tungsten leads were fusion welded to the lead selenide crystal. The capsules were sealed off at a pressure of 1 micron of Hg.

The resistivity was measured by the standard direct current method. The only modification of this technique that was made concerned the measurement of the EMF at zero current. This EMF is due to the Peltier effect and was added algebraically to the voltage drop produced when a current was passed through the specimen.

Figures 10 and 11 are curves of ρ in ohm-cm versus $10^3/T°K$. If we have a minimum in the conduction band with spherical symmetry and thus a scalar effective mass m_e, and also a single maximum with spherical symmetry in the valence band with effective hole mass m_h then

$$\rho_i = \left[e\mu_h (b+1)A\right]^{-1} T^{-3/2} \exp\left(\Delta E/2kT\right) \tag{24}$$

A first approximation assumes the bracket is a constant and the variation in $T^{-3/2}$ is small compared to the exponential term and eq (24) reduces to

$$\ln \rho_i = \ln A' + \frac{\Delta E}{2kT} \tag{25}$$

and

$$\Delta E = \frac{2kT_1T_2}{T_2 - T_1} \ln \frac{\rho_1}{\rho_2} \tag{26}$$

Results using equation (25) are.

$\Delta E = 0.417$ eV for tri-crystal

$\Delta E = 0.456$ eV for single crystal of stoichiometric PbSe.

In the case of PbSe as in the PbTe there exists a difference in the energy gap values determined optically as compared with thermal measurements, the latter yielding a higher value. For PbSe the comparable values are thermal $\sim$.45 eV, optical $\sim$.26 eV.

To see if the energy gap being measured was truly a measurement of the intrinsic value an attempt was made to quench in defects.

The only reliable data was obtained by air quenching. This involved measuring the room temperature resistivity, then bringing the specimen to equilibrium at an elevated temperature and quenching by removing the encapsuled specimen from the furnace and blowing air on the capsule. On quenching a sample from about 800°K, the resistivity after quenching was in the order of 1/3 to 1/2 the resistivity of a slow cooled specimen, clearly indicating, at least qualitatively that defect generation is responsible for some generation of carriers at elevated temperatures.

V. INVESTIGATION OF $Sn_xPb_{1-x}Te$

Specimens of ten compositions evenly spaced across the pseudobinary system $Sn_xPb_{1-x}Te$ were prepared by scaling weighed quantities of the metals into evacuated quartz capsules, and then lowering the capsules through a furnace held 50°C above the melting point at a lowering rate of 0.5 cm/hr.

Metallorgaphic examination showed that there were no second phase inclusions in the specimens, indicating that the vertical cut examined is a pseudobinary with complete miscibility of the two constituent compounds, SnTe and PbTe. Single crystals were not obtained, but rather the ingots also consisted of long thin columnar grains, the grains extending the length of the ingot, but each grain was only about 5 mm in diameter.

The resistivity of the samples was determined from 77°K to 800°K and the Hall coefficient from 77°K to 300°K.

In the intrinsic range from 77°K to 300°K, the temperature range over which the Hall coefficient was measured, the carrier concentration or all the alloys remained constant.

The resistivity was observed to increase continuously for all specimens from the lowest to highest tempera - respectively except for PbTe, which exhibited intrinsic behav. above 200°C.

Although the resistivity curves cannot be taken by themselves as definite indications of the existence or non-existence of energy gaps in these specimens, it appears as if the activation energy for carrier generation of the alloys is very low (< 0.05 eV) for specimens with tin contents greater than 15 at %. The activation energy increases approximately linearly with decreasing tin content from 15 at % to about 5 at % Sn, reaches a maximum of about 0.4 eV and then decreases to 0.35 eV for pure PbTe.

It should be emphasized that these are the values of the carrier activation energy, and not necessarily that of the energy gap, since defect formation also probably produces carriers in these alloys.

While the variation of mobility and temperature in none of the alloys obeys the standard T^n function of temperature, in general, the dependence of mobility on temperature increases with increasing tin content from roughly a $T^{-3/2}$ dependence for SnTe to a $T^{-5/2}$ dependence for PbTe.

VI. SUMMARY AND CONCLUSIONS

The disparity in energy gap values for PbTe as determined from optical and thermal measurements may be explained by generation of excess carriers due to defect generation at elevated temperatures. An analysis of activation processes involved points to Pb interstitials as the most likely defect present.

BaSe and BaTe can be prepared by direct reaction of Ba with Se and Te. The binding energies of these compounds is high as evidenced by their high melting points: BaSe ~ 1830°C, BaTe ~ 1510°C, and high resistivity at room temperature: BaSe ~ 3×10^{10} ohm cm, BaTe ~ 7×10^{7} ohm cm, indicating that both would have rather high energy gaps. On examination of the PbSe phase diagram by thermal analysis and metallographic techniques it was determined that

1) the melting point of PbSe is 678.3°C

2) a monotectic reaction occurs on the selenium rich side of PbSe

3) a monotectic reaction does not occur on the lead rich side of PbSe.

Measurements of electronic properties of PbSe indicated that

1) stoichiometric PbSe does not melt the maximum melting point but the maximum melting point occurs at a composition containing 0.009 atomic percent selenium.

2) the energy gap as determined from resistivity and Hall effect as a function of temperature, ~0.45 eV is greater than that reported from optical measurements ~ 0.26 eV.

3) on the basis of exploratory quenching experiments, it appears that the above discrepancy results from defect generation, as in the case of PbTe.

PbTe and SnTe are completely miscible in the system $Pb_xSn_{(1-x)}Te$. Preliminary experiments indicated that the electronic parameters vary continuously as Sn is substituted for Pb.

VII. REFERENCES

1. Miller, E., Komarek, K., and Cadoff, I., Trans AIME 218 979 (1960)
2. Smith, R. A., Physica 20 910 (1954)
3. Scanlon, W. W., J. Phys. Chem. Solids 8, 423 (1958)
4. Scanlon, W. W. Phys. Rev. 92 1573 (1953)
5. Hirahara, E. and Murakami, M. Phys. Soc. Jap. 9 671 (1954)
6. Gibson, A. F., Proc. Phys. Soc. 65B 378 (1952)
7. Kolomoets, N., Stavitskaya, T., Gul'bans, L. Zhur. Tekh. Fiz. 27 73 (1957)
8. Koval'chick, T. and Maslakovets, Y., Zhur. Tekh. Fiz. 26 2417 (1956)
9. Fritts, R. "Thermoelectric Materials and Devices" Reinhold Pub. 143 (1960)
10. Brebrick, R., Allgaier, R. J. Chem. Phys. 32 1826 (1960)
11. Cottrell, A. H. "Vacancies and Other Point Defects in Metals and Alloys" Institute of Metals (1958) p1
12. Fritts, R. W. and Karrer, S. Bull. Am. Phys. Soc. 1, 226 (1956)
13. Boltaks, S. B. and Makhov, Y. Zhur. Tekh. Fix. 28, 1046 (1958)
14. Kroger, F. A. and Vink, H. J. "Solid State Physics" Academic Press Vol. 3, p. 260 1955
15. Brouwer, G. Phil. Res. Rep. 9, 336 (1954)
16. Goldschmidt, V. M.: Geochemisch. Verteil sgesetla VII, 1927.
17. Cadoff, I. and Nielsen, J., AIME Trans., 1953, vol. 197, p. 248.
18. Pell, E. M., Phys. Rev. 87, 457 (1952)
19. Zollweg, R. J , Phys. Rev., 1958, vol. 111, p. 113
20. Nozato, R., and Igaki, K., Bull. Maniwa Univ. (Japan),A3, 1955
21. Pelabon, H., Compt. rend., 144, 1907, 1159-1161
22. Friedrich, K., and Leroux, A., Metallurgie, 5, 1908, 355-358

23. Hansen, M. and Anderko, K., "Constitution of Binary Alloys," McGraw-Hill, 1958. 1110-1112

24. Goldberg, A. E. and Michell, G. R., J. Chem. Phys. 22, 220-222, 1954

25. Putley, E. H., Proc. Phys. Soc. (London), 65B, 338, 1952.

26. Putley, E. H., Proc. Phys. Soc. (London), 65B, 993, 1952

Additional Publications Based on Work on Contract AF 33(616)-3883

Miller, E., Komarek, K., and Cadoff, I. Trans AIME 215 882 1959
Miller, E., Komarek, K., and Cadoff, I. Trans AIME 218 382 1960

TABLE I

LIQUIDUS DATA

Composition Atomic Percent	Average Cooling Rate °C Per Min	Liquidus Temperature (°C)	Average Liquidus (°C) Temperature
30.00 Se 70.00 Pb	1°C/Min	970.45	970.45°C
35.00 Se 65.00 Pb	1.2 0.9	981.84 982.26	982.1
40.00 Se 59.99 Pb	0.6 0.8 0.8	1006.1 1006.3 1006.1	1006.2
45.00 Se 55.00 Pb	1.3 1.1	1036.0 1035.7	1035.9
47.00 Se 53.00 Pb	0.6 0.6	1059.1 1059.7	1059.4
48.00 Se 52.00 Pb	0.8	1070.7	1070.7
49.00 Se 51.00 Pb	1.1 1.1	1077.3 1077.9	1077.6
49.16 Se 50.84	0.9	1078.5	1078.5
50.00 Se 50.00 Pb	1. 0.6 1.2	1080.9 1080.4 1080.9	1080.7
50.99 Se 49.01 Pb	1.3	1079.9	1079.9
52.01 Se 47.99 Pb	1.0 0.65	1069.3 1069	1069.5
53.00 Se 47.00	0.7	1048..	1048.1
56.00 Se 44.00 Pb	0.5 0.6 0.5	1011.7 1012.2 1010.7	1011.5
65.00 Se 40.00 Pb	0.6 0.5	943.5 943.4	943.5
65.00 Se 35.00 Pb	0.8	853.5	853.5
70.00 Se 30.00 Pb	0.93	778.7	778.7

TABLE II

MONOTECTIC DATA - SELENIUM RICH SIDE

Composition Atomic Percent	Average Cooling Rate °C	Temperature of Monotectic Arrest °C
65.00 Se 35.00 Pb	0.83	678.53
70.00 Se 30.00 Pb	0.6 0.7	678.1 678.1
60.00 Se 40.00 Pb	0.5 0.6	678.2 678.2
For Monotectic Occuring at 76.5 at. % Se		Av. Temp. 678.3°C

TABLE III

ALLOYS INVESTIGATED FOR MONOTECTIC ARREST - LEAD RICH SIDE

Atomic Percent Pb	Average Cooling Rate °C/Min	Average Liquidus Temp °C
79.50	0.75	926.0
75.00	0.85	952.4
70.00	1.1	969.1
65.00	1.0	982.1
59.99	0.8	1006.2

TABLE IV

ELECTRONIC DATA FOR DEVIATION OF MAXIMUM MELTING POINT FROM STOICHIOMETRIC COMPOSITION FOR PbSe

Liquid Composition Atomic Percent Excess Lead	Average Seed ρ Resistivity Ohm	Holes / Cm^3	%Hole Atom
0.00	0.0019	$5.9 \cdot 10^{18}$	0.017
0.02	0.0025	$4.5 \cdot 10^{18}$	0.013
0.03	0.0045	$2.5 \cdot 10^{18}$	0.0072

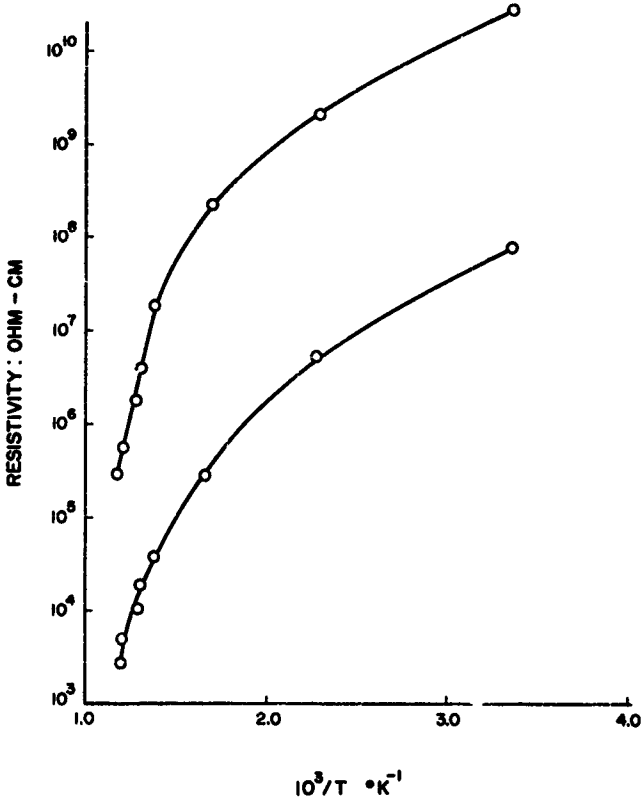

Figure 1. Resistivity versus Temperature for BaTe and BaSe.

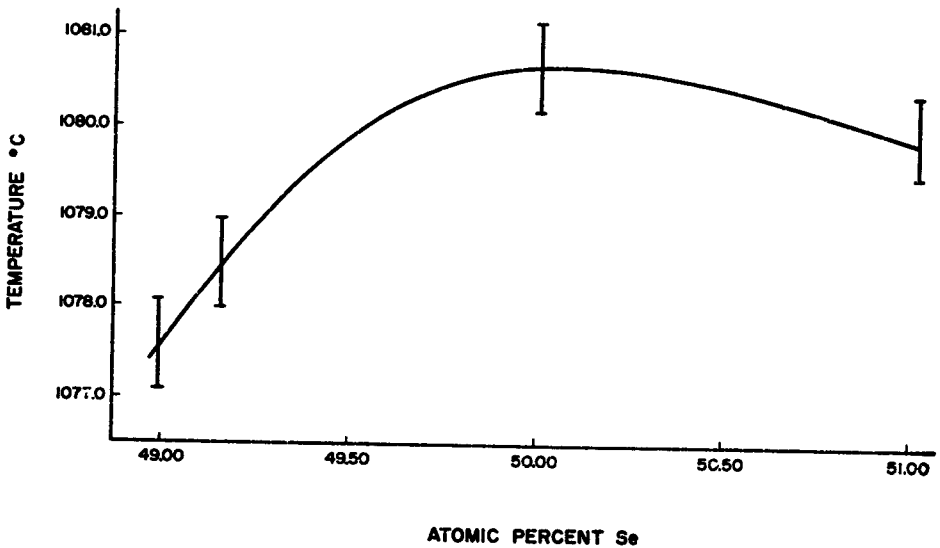

Figure 2. Temperature versus Atomic % Se in the Stoichiometric Point Region

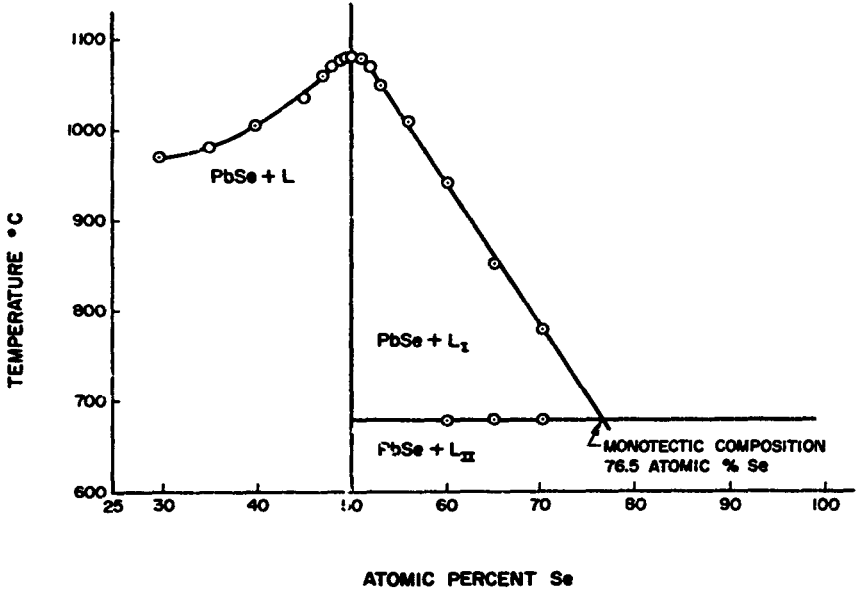

Figure 3. Partial Pb-Se Phase Diagram

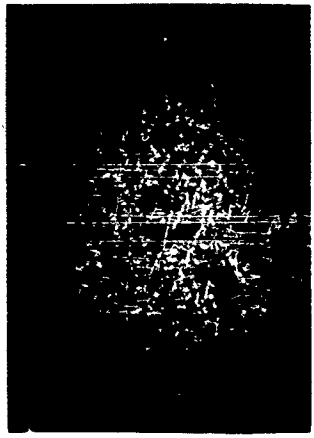

Figure 4 - 14%Se 86%Pb (At.%). Air quenched from 1000°F. C30 under polarized light.

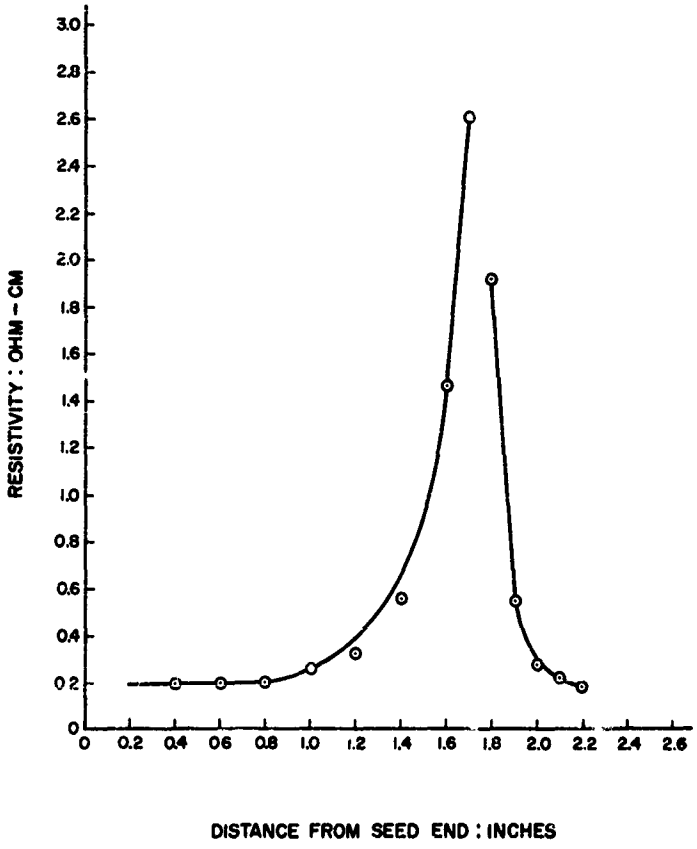

Figure 5. Resistivity Scan Stoichiometric PbSe Single Crystal

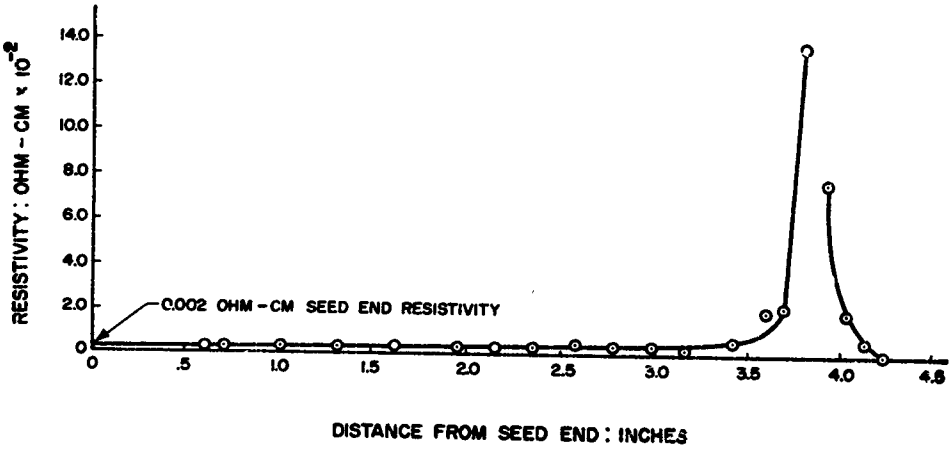

Figure 6. Resistivity Scan 0.02 Excess Pb, PbSe Single Crystal

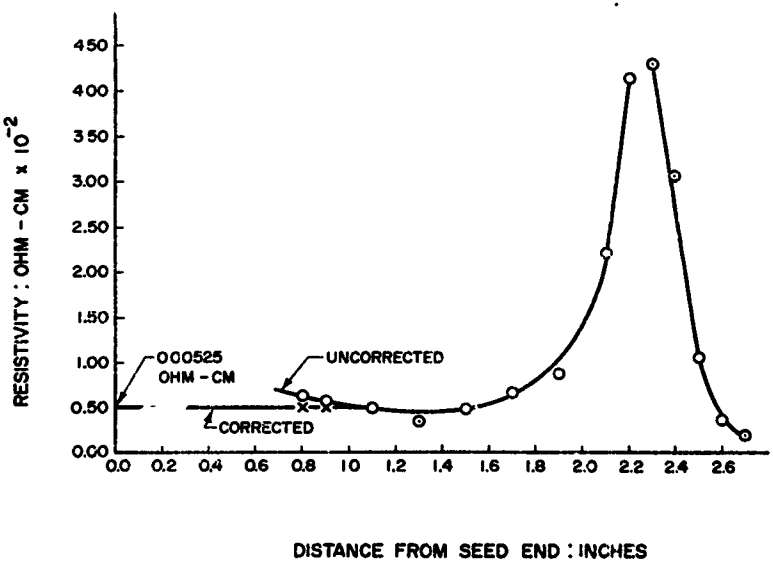

Figure 7. Resistivity Scan 0.03 Excess Pb, PbSe Single Crystal

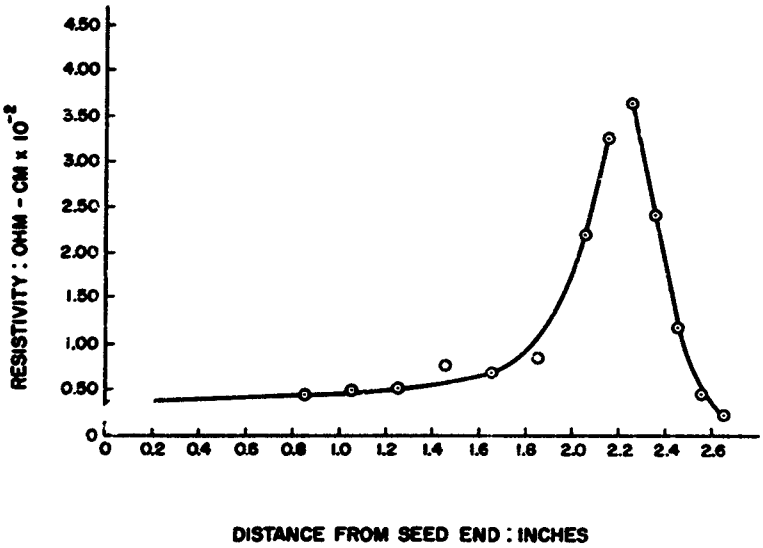

Figure 8. Resistivity Scan 0.03 Excess Lead, PbSe Single Crystal

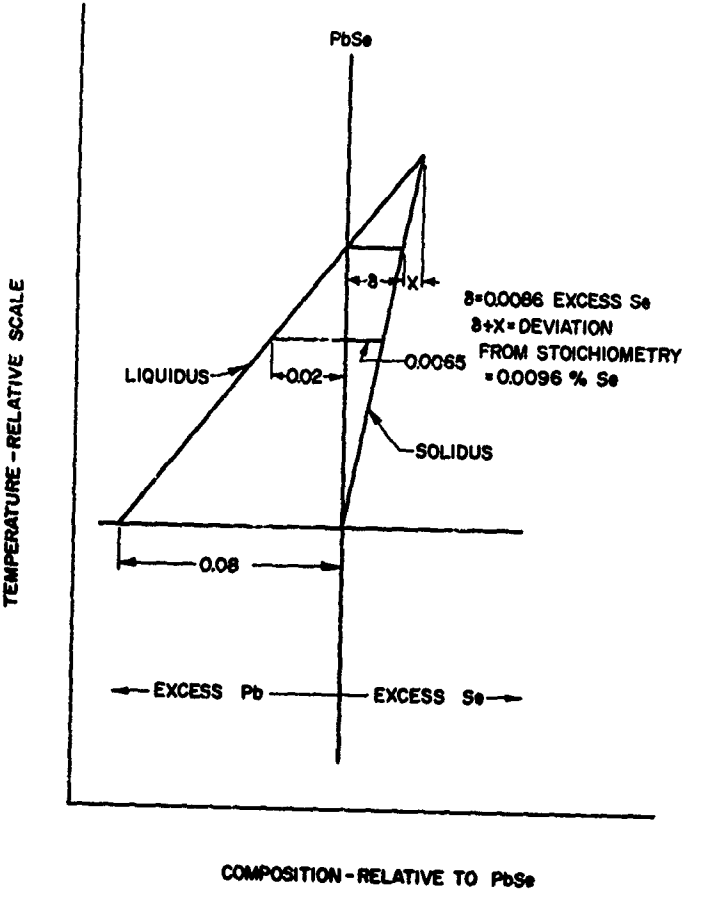

Figure 9. Partial Pb-Se Phase Diagram in the Vicinity of the Stoichiometric Composition

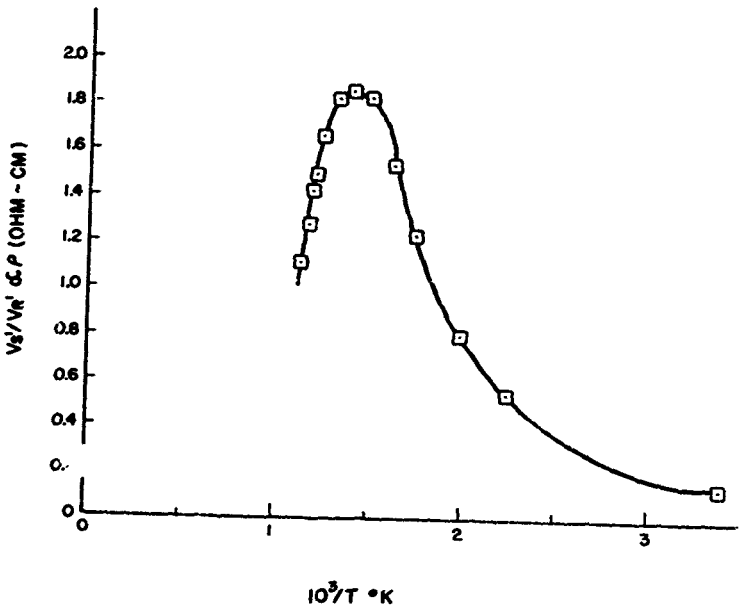

Figure 10. Resistivity versus $10^3/T°K$, Single Crystal, Stoichiometric PbSe

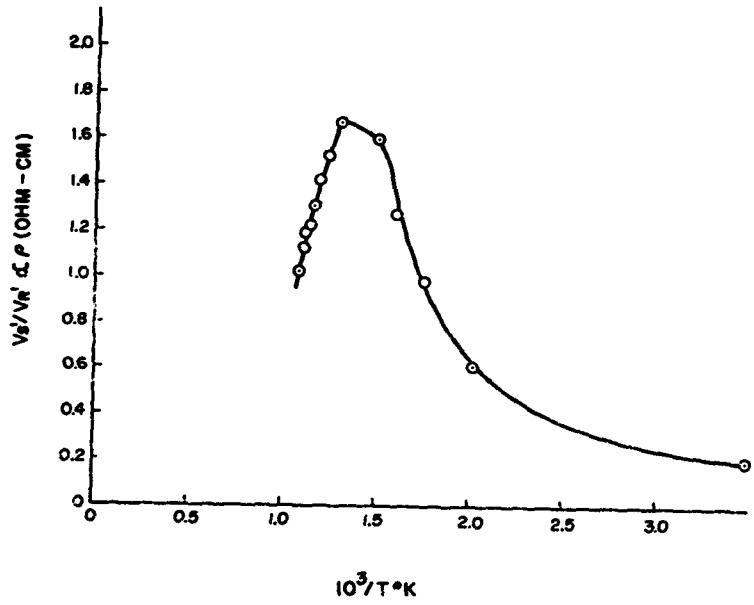

Figure 11. Resistivity versus $10^3/T^\circ K$, Tri-Crystal PbSe, N-Type

AD-

NEW YORK UNIVERSITY, NEW YORK, N Y ELECTRONIC PROPERTIES OF SOME INTERMETALLIC COMPOUNDS, by E Miller, D Seidman, K Komarek and I Cadoff Dec 1961 34 p incl illus tables (Proj 7201; Task 70661) ARL 131 (Contract AF 33(616)-3883)

Unclassified report

Additional analysis of the data for the PbTe system shows that the disparity in energy gap values for PbTe as determined from optical and thermal measurements may be explained by generation of excess carriers due to defect generation at elevated temperatures An analysis of activation processes involved points to Pb interstitials as the most likely defect present

BaSe and BaTe can be prepared by direct reaction of Ba with Se and Te The binding energies o these compounds is high as evidenced

UNCLASSIFIED

AD-

by their high melting points: BaSe~1870°C, BaTe~1510°C, and high resistivity at room temperature: BaSe~3 x 10^{10} ohm cm, BaTe 7 x 10^{7} ohm cm, indicating that both would have rather high energy gaps

Investigation of the PbSe system resulted some revisions in the phase diagram The electronic properties indicate that a deviation between stoichiometry and maximum melting exists and that, as in the case of PbTe, there is a difference in the thermal and optical energy gaps

PbTe and SnTe are completely miscible in the system $Pb_xSn_{(1-x)}Te$ Preliminary experiments indicated that the electronic parameters vary continuously as Sn is substituted for Pb.

UNCLASSIFIED

AD-

NEW YORK UNIVERSITY, NEW YORK, N Y ELECTRONIC PROPERTIES OF SOME INTERMETALLIC COMPOUNDS, by E Miller, D Seidman, K Komarek and I Cadoff Dec 1961 34 p incl illus tables (Proj 7201, Task 70661) ARL 131 (Contract AF 33(616)-3883)

Unclassified report

Additional analysis of the data for the PbTe system shows that the disparity in energy gap values for PbTe as determined from optical and thermal measurements may be explained by generation of excess carriers due to defect generation at elevated temperatures An analysis of activation processes involved points to Pb interstitials as the most likely defect present

BaSe and BaTe can be prepared by direct reaction of Ba with Se and Te The binding energies of these compounds is high as evidenced

UNCLASSIFIED

AD-

by their high melting points: BaSe~1870°C, BaTe~1510°C, and high resistivity at room temperature: BaSe~3 x 10^{10} ohm cm, BaTe 7 x 10^{7} ohm cm, indicating that both would have rather high energy gaps

Investigation of the PbSe system resulted in some revisions in the phase diagram The electronic properties indicate that a deviation between stoichiometry and maximum melting exists and that, as in the case of PbTe, there is a difference in the thermal and optical energy gaps

PbTe and SnTe are completely miscible in the system $Pb_xSn_{(1-x)}Te$ Preliminary experiments indicated that the electronic parameters vary continuously as Sn is substituted for Pb.

UNCLASSIFIED